Inorganic Chemistry

Article

pubs.acs.org/IC

Abrupt Spin Transition with Thermal Hysteresis of Iron(III) Complex $[Fe^{III}(Him)_2(hapen)]AsF_6$ (Him = Imidazole, H_2hapen = *N,N′*-Bis(2-hydroxyacetophenylidene)ethylenediamine)

Takeshi Fujinami,[†] Masataka Koike,[†] Naohide Matsumoto,*[,†] Yukinari Sunatsuki,[‡] Atsushi Okazawa,[§] and Norimichi Kojima[§]

[†]Department of Chemistry, Faculty of Science, Kumamoto University, Kurokami 2-39-1, Kumamoto 860-8555, Japan

[‡]Department of Chemistry, Faculty of Science, Okayama University, Tsushima-naka 1-1, Okayama 700-8530, Japan

[§]Department of Basic Science, Graduate School of Arts and Sciences, The University of Tokyo, Komaba 3-8-1, Meguro-ku, Tokyo 153-8902, Japan

Supporting Information

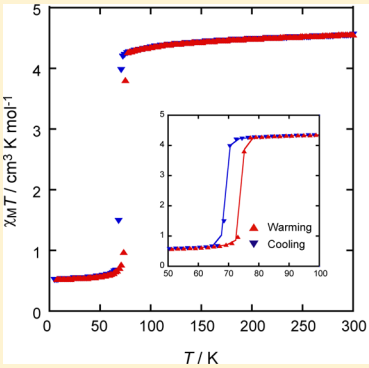

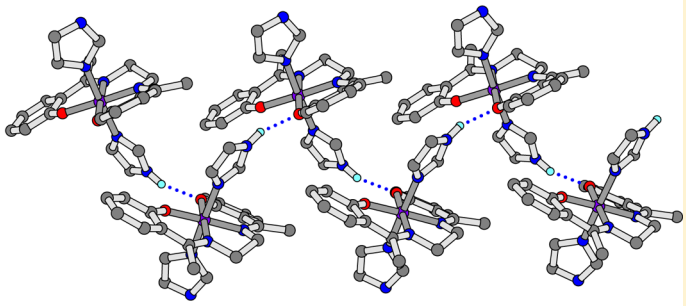

ABSTRACT: The solvent-free spin crossover iron(III) complex $[Fe^{III}(Him)_2(hapen)]AsF_6$ (Him = imidazole, H_2hapen = *N,N′*-bis(2-hydroxyacetophenylidene)ethylenediamine), exhibiting thermal hysteresis, was synthesized and characterized. The Fe^{III} ion has an octahedral coordination geometry, with N_2O_2 donor atoms of the planar tetradentate ligand (hapen) and two nitrogen atoms of two imidazoles at the axial positions. One of two imidazoles is hydrogen-bonded to the phenoxo oxygen atom of hapen of the adjacent unit to give a hydrogen-bonded one-dimensional chain, while the other imidazole group is free from hydrogen bonding. The temperature dependencies of the magnetic susceptibilities and Mössbauer spectra revealed an abrupt spin transition between the high-spin (S = 5/2) and low-spin (S = 1/2) states, with thermal hysteresis.

INTRODUCTION

The high-spin (HS) and low-spin (LS) states of the spin crossover (SCO) complex are interconvertible by external physical perturbations such as temperature, pressure, and light irradiation.[1] While SCO behavior originates from the phenomenon of a single molecule, SCO properties such as steepness, multistep SCO, hysteresis, and light-induced excited spin state trapping (LIESST) result from the cooperative effect. Mainly three synthetic strategies have been employed to achieve the cooperative effect: (1) covalent linker (bridging ligand) to form coordination polymers,[2] (2) $\pi-\pi$ stacking among the SCO sites,[3] and (3) hydrogen bonding.[4] Among SCO compounds, Fe^{II} and Fe^{III} compounds have been the most intensively studied. A number of SCO Fe^{II} compounds showed abrupt spin transitions exhibiting thermal hysteresis, while SCO Fe^{III} compounds generally exhibit gradual spin equilibrium and show no thermal hysteresis except for several compounds with $\pi-\pi$ stacking.[3c]

Weber reported an SCO Fe^{II} complex $[Fe^{II}L(Him)_2]$ (L is a Jäger-type N_2O_2 Schiff-base ligand,[5] and Him is imidazole) exhibiting a hydrogen-bonded 2D network structure and a 70 K wide thermal hysteresis around room temperature.[6] This result demonstrates the high potential of H-bonds for transmitting cooperative interactions for SCO phenomenon and suggests a possibility of SCO Fe^{III} compound with thermal hysteresis when the network of the H-bonds is well-organized. We have been interested in the importance of hydrogen bond for SCO properties and reported that the H bonds can modify the SCO profile[4] and give an effective cooperativity even for SCO Fe^{III} complexes.[7] In this study, we report the first SCO Fe^{III} complex of salen-type N_2O_2 tetradentate ligand and two imidazoles with a small thermal hysteresis. A family of Fe^{III} complexes with salen-type N_2O_2 ligands and two axial monodentate ligands was first synthesized by Nishida, and he showed that the spin states

Received: November 27, 2013
Published: February 5, 2014

   dx.doi.org/10.1021/ic402947u | Inorg. Chem. 2014, 53, 2254−2259

can be tuned primarily by the total ligand field strength provided by the equatorial and axial ligands.[8] It has been known for a long time that the Fe sites in some heme proteins exhibit SCO behavior,[9] which plays a key role in their biological functions. From the viewpoint of developing a model compound of heme proteins, a number of iron porphyrins have been studied.[10] Nishida studied his compounds as a simple model compound of the Fe sites in some heme proteins. Later, Matsumoto,[11] Murray,[12] and Real[13] reported the SCO Fe^{III} complexes with analogous N_2O_2 Schiff-base ligands, and they revealed the relevant factors to determine the SCO properties, while the SCO with hysteresis has not been observed for these complexes. In our previous paper,[14] we reported Fe^{III} complexes $[Fe^{III}(Him)_2(hapen)]Y\cdot solvent$ (Y = various anions, including BPh_4^-, $CF_3SO_3^-$, PF_6^-, ClO_4^-, and BF_4^-), where the equatorial N_2O_2 Schiff-base ligand (H_2hapen = *N*,*N*′-bis(2-hydroxyacetophenylidene)ethylenediamine) and the two axial ligands are fixed and the counteranion is varied. These complexes showed three types of assembly structures constructed of imidazole···phenoxo hydrogen bonds, consisting of "linear dimers," "cyclic dimers," and "one-dimensional (1D) chains." Among them, the PF_6^- salt with 1D chain showed an abrupt spin transition, and its magnetic behavior is unusual for SCO Fe^{III} complexes reported so far. In this study, the AsF_6^- salt, with anion size than larger that of PF_6^-, was synthesized in the hope of the appearance of hysteresis, and the resulting structure and magnetic property were investigated. As anticipated, this complex showed an abrupt spin transition with thermal hysteresis. We report here the synthesis, structure, magnetic property, and Mössbauer spectroscopy.

EXPERIMENTAL SECTION

Materials. All reagents and solvents used in this study are commercially available from Tokyo Kasei Co., Ltd., Tokyo, Japan and Wako Pure Chemical Industries, Ltd., Osaka, Japan and were used without further purification. All synthetic procedures were carried out in an open atmosphere.

Ligand (H_2hapen) and Precursor Iron(III) Complex ($[Fe^{III}Cl(hapen)]\cdot 0.5CH_3OH$). The tetradentate ligand H_2hapen was prepared according to the literature.[15] Yellow crystalline material. Yield: 99%. Anal. Calcd for H_2hapen ($C_{18}H_{20}N_2O_2$): C, 72.95; H, 6.80; N, 9.45%. Found: C, 72.93; H, 6.82; N, 9.32%. mp =193 − 196 °C. The precursor iron(III) complex $[Fe^{III}Cl(hapen)]\cdot 0.5CH_3OH$ was prepared according to the literature reported previously.[14b] To a solution of H_2hapen (10 mmol, 2.96 g) in 100 mL of methanol was added anhydrous $Fe^{III}Cl_3$ (10 mmol, 1.62 g), and the resulting solution was warmed for 30 min on a hot plate. To the solution was added a solution of triethylamine (20 mmol, 2.00 g) drop-by-drop. Black crystals were collected by suction filtration and washed with diethyl ether. Anal. Calcd for $[Fe^{III}Cl(hapen)]\cdot 0.5CH_3OH$ ($C_{18}H_{18}N_2O_2FeCl\cdot 0.5CH_3OH$): C, 55.32; H, 5.02; N, 6.97%. Found: C, 55.29; H, 4.72; N, 7.26%.

$[Fe^{III}(Him)_2(hapen)]AsF_6$. To a suspension of $[Fe^{III}Cl(hapen)]\cdot 0.5CH_3OH$ (0.50 mmol, 0.20 g) in 15 mL of methanol was added an excess amount of imidazole (5.0 mmol, 0.34 g), and the mixture was stirred for 15 min on a hot-plate and then filtered. To the filtrate was added a solution of $NaAsF_6$ (0.50 mmol, 0.13 g) in 5 mL of methanol. The resulting solution was allowed to stand for a few days, during which time black platelike crystals precipitated; the crystals were collected by suction filtration and washed with diethyl ether. Yield: 0.107 g (32%). Anal. Calcd for $[Fe^{III}(Him)_2(hapen)]AsF_6$ ($C_{24}H_{26}N_6O_2Fe\cdot AsF_6$): C, 42.69; H, 3.88; N, 12.45%. Found: C, 42.49; H, 3.90; N, 12.54%.

Physical Measurements. Elemental analyses (C, H, and N) were carried out by Miss Kikue Nishiyama at the Center for Instrumental Analysis of Kumamoto University. Magnetic susceptibilities were measured by a Quantum Design MPMS-XL5 magnetometer in the temperature range of 5−300 K at the sweeping rate of 0.5 K min^{-1} under an applied magnetic field of 0.5 T. The magnetic susceptibilities were measured while lowering the temperature from 300 to 5 K in the first run. Subsequently, the magnetic susceptibilities were measured while raising the temperature from 5 to 300 K in the second run. The calibration was performed with palladium metal. Corrections for diamagnetism were applied using Pascal's constants.[16] For the ^{57}Fe Mössbauer spectroscopic measurement, ^{57}Co in Rh was used as a Mössbauer source. The spectra were calibrated by using the six lines of a body-centered cubic iron foil (α-Fe), the center of which was taken as zero isomer shift. Mössbauer spectra were fitted with a MossWinn 3.0 program.[17]

X-ray Crystallography. X-ray diffraction data were collected using a Rigaku RAXIS RAPID imaging plate diffractometer using graphite monochromated Mo Kα radiation (λ = 0.71073 Å). The temperature of the crystal was maintained at the selected temperature by means of a Rigaku cooling device. The X-ray diffraction data for $[Fe^{III}(Him)_2(hapen)]AsF_6$ were collected at 200 K. The data were corrected for Lorentz, polarization, and absorption effects. The structure was solved by a direct method and expanded using the Fourier technique.[18] Hydrogen atoms were fixed at the calculated positions and refined using a riding model. All calculations were performed using the CrystalStructure crystallographic software package.[19]

RESULTS AND DISCUSSION

Synthesis and Characterization of $[Fe^{III}(Him)_2(hapen)]AsF_6$. In 1975, Nishida reported SCO Fe^{III} compounds with salen-type N_2O_2 Schiff-base ligand and two imidazoles $[Fe^{III}(Him)_2(salen\text{-}type)]^+$, where the SCO behaviors were gradual.[8] Later Matsumoto,[11] Murray,[12] and Real[13] synthesized SCO Fe^{III} complexes with analogous Schiff-base ligands. In our previous paper,[14] Fe^{III} complexes with the formula of $[Fe^{III}(Him)_2(hapen)]Y\cdot solvent$ were synthesized by varying the counteranion Y (Y = BPh_4^-, $CF_3SO_3^-$, PF_6^-, ClO_4^-, and BF_4^-), where the equatorial N_2O_2 Schiff-base ligand (H_2hapen) and axial imidazoles (Him) were fixed. These complexes showed three types of assembly structures constructed of imidazole···phenoxo hydrogen bonds, consisting of linear dimers, cyclic dimers, and 1D chains. Among them, the PF_6^- salt exhibiting hydrogen-bonded 1D chain structure showed an abrupt spin transition, and its magnetic behavior is unusual for SCO Fe^{III} complex. On the basis of that result, we focused on the large-sized AsF_6^- salt in the hope of realizing an abrupt SCO and thermal hysteresis. The complex $[Fe^{III}(Him)_2(hapen)]AsF_6$ was obtained as black platelike crystals from the mixed solution of $[Fe^{III}Cl(hapen)]\cdot 0.5CH_3OH$, imidazole, and $NaAsF_6$ in a 1:10:1 molar ratio in methanol, according to the similar method applied for the other salts.[14] The C, H, and N elemental analyses agreed with the formula $[Fe^{III}(Him)_2(hapen)]AsF_6$, demonstrating no existence of any crystal solvents. The ground sample of the AsF_6^- salt showed no thermochromism, suggesting the spin transition occurs in a temperature region lower than that of liquid nitrogen, as

dx.doi.org/10.1021/ic402947u | Inorg. Chem. 2014, 53, 2254−2259

confirmed later by the magnetic susceptibility measurements, while the SbF_6^- salt with larger anion size exhibited thermochromism, from dark reddish violet at ambient temperature to dark black green at liquid nitrogen temperature, demonstrating a spin crossover of Fe^{III} complex with Schiff-base ligand of N_4O_2 donor atoms.

Crystal Structure of $[Fe^{III}(Him)_2(hapen)]AsF_6$ in the HS State. The single-crystal X-ray structure was determined at 200 K. The crystallographic data are listed in Table 1. Relevant coordination bond distances, angles, and hydrogen-bond distances are given in Table 2. The complex crystallized into a monoclinic space group $C2/c$, and its unique unit consists of one cation $[Fe^{III}(Him)_2(hapen)]^+$ and one counteranion AsF_6^-. The molecular structure of the $[Fe^{III}(Him)_2(hapen)]^+$ part with the atom numbering scheme is shown in Figure 1a,b. The Fe^{III} ion has an octahedral coordination environment with the N_2O_2 donor atoms of electronically dinegative tetradentate ligand hapen at the equatorial sites and the N_2 donor atoms of two imidazoles at the two axial positions. The four Fe−N bond distances are in the range of 2.096(9)−2.139(7) Å, in which the Fe−N(imidazole) distance is slightly longer than the Fe−N(imine) distance. The Fe−O1 distance of 1.886(6) Å is slightly shorter than the Fe−O2 distance of 1.904(8) Å, where O2 is hydrogen-bonded to N6* (*; 1/2 − x, 1/2 + y, 1/2 − z) of the imidazole group of the adjacent cation complex and O1 is free from hydrogen bonding. These Fe−N and Fe−O coordination bond distances at 200 K are consistent with the bond distances reported for HS Fe^{III} complexes with similar Schiff-base ligands. The O1−Fe−O2 bond angle of 101.3(3)° is indicative of the HS spin state at 200 K on the basis of the structural parameters of the analogous $[Fe^{III}(Him)_2(hapen)]^+$,[14] where HS compounds have the large angle around 104°, while SCO compounds have smaller angle around 101°. Figure 1b shows the orientations of the two imidazole rings, in which one imidazole ring bisects the angles defined by the two N−Fe−O diagonals, and the other imidazole ring is oriented nearly along the N−Fe−O diagonal. The five-membered chelate ring involving ethylenediamine moiety assumes a gauche conformation, in which C9 and C10 atoms are deviated by −0.19 and +0.39 Å, respectively, from the plane defined by Fe, N1, and N2 atoms. The dihedral angle between the N_2O_2 coordination plane and the benzene moiety is −10.1° and 22.4° for benzene rings A and B, respectively, in which the ring B bound to O2 is much tilted. Murray et al. demonstrated that the present type of distortion of two benzene moieties makes the spin transition possible.[12]

Figure 2a,b shows the 1D zigzag-chain structure of $[Fe^{III}(Him)_2(hapen)]^+$. The 1D structure is constructed by intercation hydrogen bonding between phenoxo oxygen O2 and imidazole nitrogen N6* of the adjacent cation complex, whose hydrogen bond distance is O2···N6* = 2.808(9) Å. The adjacent cation complexes, linked by the hydrogen bond, are related by a 2-fold screw axis along the b-axis, and the O2···N6* hydrogen bond is repeated to form a 1D structure running along the b-axis. The remaining imidazole nitrogen atom N4 of the two imidazoles of one cation is close to the F3 and F9 atoms of the AsF_6^- ion, with N4···F3 = 3.02(2) and N4···F9 = 2.94(2) Å. However, as the occupancy factor of 0.5 was adapted

Table 1. Crystallographic Data

formula	$C_{24}H_{26}N_6O_2FeAsF_6$
formula weight	675.27
crystal system	monoclinic
space group	$C2/c$ (No.15)
T, K	200
a, Å	24.236(3)
b, Å	9.5662(8)
c, Å	24.599(3)
β, deg	112.342(3)
V, Å^3	5274.9(9)
Z	8
D_{calcd}, g cm^{-3}	1.700
μ, mm^{-1}	1.894
R^a, Rw^b	0.0796, 0.2453

$^aR = \sum||F_o| - |F_c||/\sum|F_o|$. $^bRw = [\sum w(|F_o^2| - |F_c^2|)^2]/\sum w|F_o^2|^2]^{1/2}$.

Table 2. Coordination Bond Distances (Å), Bond Angles (deg), and Hydrogen Bond Distances (Å) at 200 K

bond lengths (Å)			
Fe−N1	2.096(9)	Fe−O1	1.886(6)
Fe−N2	2.109(7)	Fe−O2	1.904(8)
Fe−N3	2.133(6)		
Fe−N5	2.139(7)		
average ⟨Fe−N⟩	2.119	average ⟨Fe−O⟩	1.895
bond angles (deg)			
O1−Fe−O2	101.3(3)	N1−Fe−N3	89.5(3)
O1−Fe−N1	89.2(3)	N1−Fe−N5	87.7(3)
O2−Fe−N2	89.6(3)	N2−Fe−N3	88.3(3)
N1−Fe−N2	79.9(3)	N2−Fe−N5	85.2(3)
hydrogen bond lengths (Å)			
N6H···O2*	2.808(9)	N6H···O1*	3.257(12)

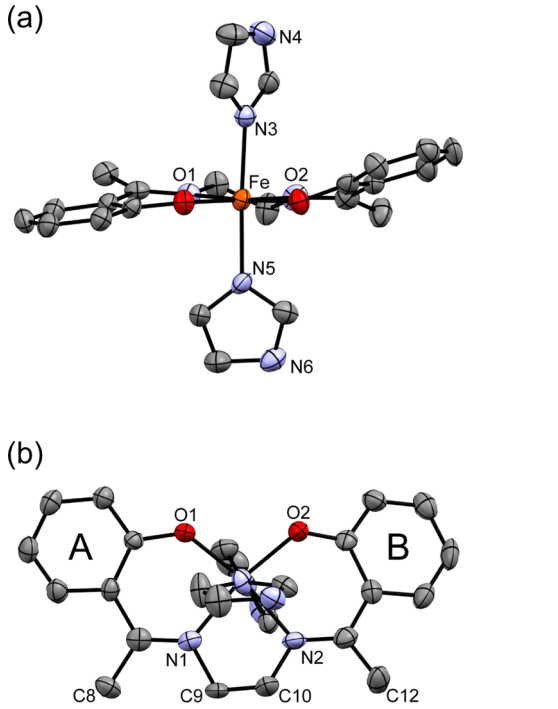

Figure 1. (a) ORTEP drawing of the $[Fe^{III}(Him)_2(hapen)]^+$ cation of $[Fe^{III}(Him)_2(hapen)]AsF_6$, with the selected atom numbering at 200 K, showing the distorted orientation of two benzene rings. The thermal ellipsoids were drawn at the 50% probability level. (b) View of the cation complex projected on the planar tetradentate Schiff-base ligand, showing the orientations of two imidazole rings.

dx.doi.org/10.1021/ic402947u | Inorg. Chem. 2014, 53, 2254−2259

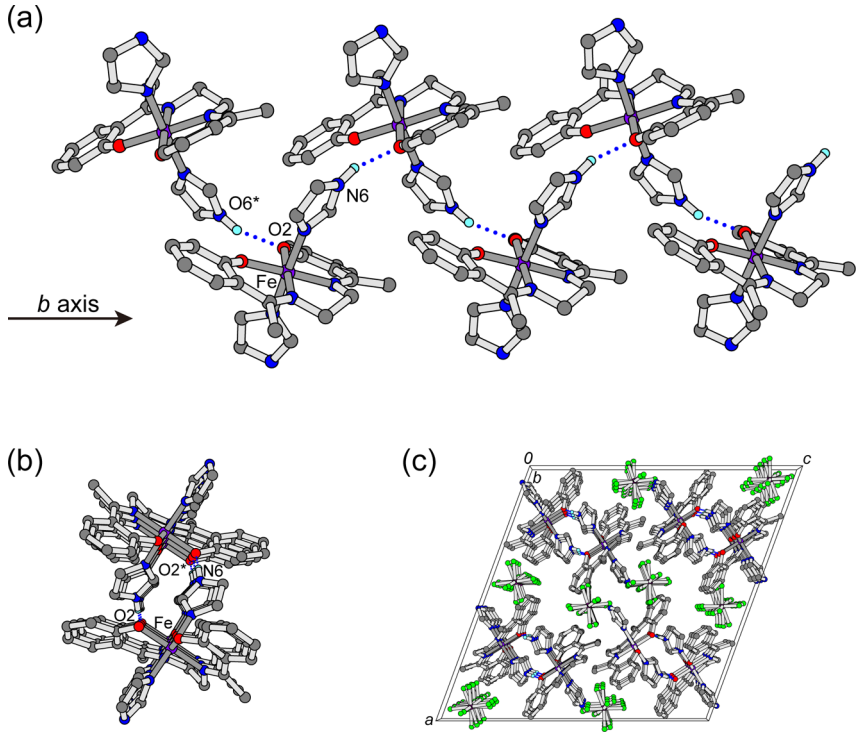

Figure 2. (a) 1D zigzag-chain structure constructed by the intercation hydrogen bonds running along the *b*-axis. (b) 1D structure projected along the *b*-axis. (c) Packing diagram projected on the *ac* plane.

for F3 and F9 due to the disorder of the AsF_6^- anion, and the angles of N4−H···F3 = 114.1(7) and N4−H···F3 = 111.9(7)° are far from 180°, it can be considered that the interaction between the imidazole nitrogen atom N4 and the anion is very weak even if it exists. Figure 2c shows a packing diagram for $[Fe^{III}(Him)_2(hapen)]AsF_6$, in which 1D chains of $\{[Fe^{III}(Him)_2(hapen)]^+\}_\infty$ are arrayed along the *b*-axis and the anions of AsF_6^- occupy the space among the 1D chains. The interaction among AsF_6^- anions and the 1D chains must be weak even if it exists. The 1D chain can be described as a spring.

Magnetic Properties. The molar magnetic susceptibilities (χ_M) of the polycrystalline samples were measured in the temperature range of 5−300 K, under an applied magnetic field of 0.5 T, and at a sweep rate of 0.5 K min^{-1}. The magnetic susceptibility was measured on lowering the temperature from 300 to 5 K as the first run and subsequently on elevating the temperature from 5 to 300 K as the second run. The plots of $\chi_M T$ versus T are given in Figure 3, showing a complete abrupt spin transition between the HS (S = 5/2) and LS (S = 1/2) states. On lowering the temperature from 300 to 5 K in the first run, the $\chi_M T$ value at temperature higher than ca. 80 K assumes a plateau value of ca. 4.5 cm^3 mol^{-1} K, whose value is consistent with 4.377 cm^3 mol^{-1} K of the spin-only HS value (S = 5/2) with g = 2.00. The $\chi_M T$ value in the lower-temperature region (<50 K) assumes a plateau value of ca. 0.5 cm^3 mol^{-1} K, which is slightly larger than the 0.375 cm^3 mol^{-1} K value of the spin-only LS value (S = 1/2) with g = 2.00 but is comparable to those of the reported LS Fe^{III} complexes. On lowering the temperature from 300 to 5 K, the $\chi_M T$ value keeps the constant in the temperature region higher than 80 K, decreases abruptly around ca. 68 K, and then reaches a constant value in the temperature region lower than 60 K. The spin-transition temperature in the cooling mode is evaluated at $T_{1/2}\downarrow$ = 69.4 K.

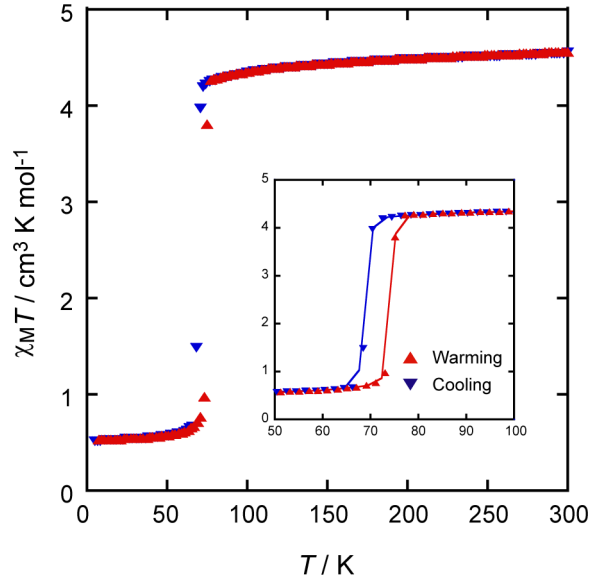

Figure 3. $\chi_M T$ vs T plots for $[Fe^{III}(Him)_2(hapen)]AsF_6$ in the temperature region of 5 to 300 K. (inset) $\chi_M T$ vs T plots in the temperature region between 50 and 100 K, showing hysteresis.

On elevating the temperature from 5 to 300 K in the second run, the spin transition occurs at a higher temperature of $T_{1/2}\uparrow$ = 74.0 K than $T_{1/2}\downarrow$ = 69.4 K of the first run, as seen in the inset. Thus, the width of thermal hysteresis is 4.6 K.

Mössbauer Spectra. To clarify microscopically the spin states at various temperatures, we performed ^{57}Fe Mössbauer measurements, as shown in Figure S1 (Supporting Information). The Mössbauer spectra were recorded at 7, 50, 70, 71, 72, 73, 100, and 200 K in cooling and warming processes. A deconvolution analysis of each spectrum successfully gave the

dx.doi.org/10.1021/ic402947u | Inorg. Chem. 2014, 53, 2254−2259

appropriate Mössbauer parameters and the molar fraction of the HS and LS states (Supporting Information, Table S1).

At 200 K, a doublet was observed with the isomer shift (δ) of 0.47 mm s^{-1} and the quadrupole splitting (ΔE_Q) of 1.34 mm s^{-1}, which is attributable to a HS Fe^{III} species. With decreasing temperature, a wider doublet, which can be attributed to the LS Fe^{III} state (δ = 0.09−0.20 mm s^{-1}, ΔE_Q = 1.99−2.21 mm s^{-1}) appeared and gradually increased as the temperature approached 72 K. On further cooling, the intensity of the HS doublet abruptly decreased, in contrast with the growth of the LS doublet, corresponding to the spin-crossover transition. The HS doublet disappeared below 50 K, indicating the complete spin conversion.

In warming mode, the spin conversion from the LS to the HS state was observed with a thermal hysteresis (ca. 1 K), which is compatible with the magnetic susceptibility data. As shown in Figure 4a,b, the spectrum at 71 K in warming mode consists of

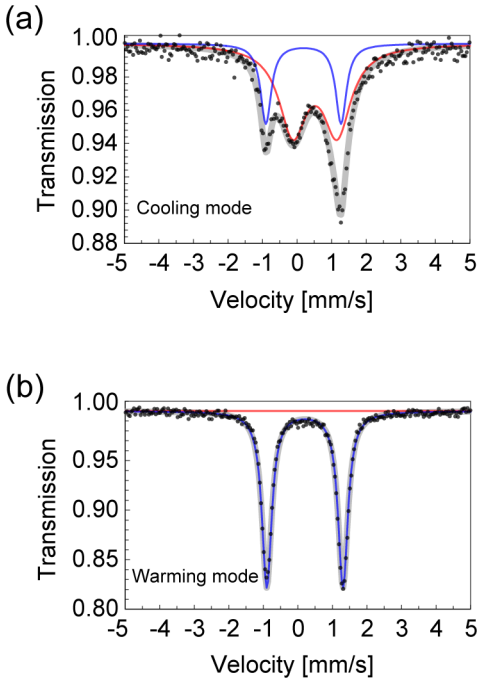

Figure 4. Selected Mössbauer spectra at 71 K upon (a) gradual cooling from room temperature and (b) gradual warming from 7 K. The transmission at the *y*-axis is taken.

a doublet attributable to LS Fe^{III} species, while the spectrum at 71 K in cooling mode consists of two doublets attributable to HS and LS Fe^{III} species with the relative fraction of HS/LS = 73.6:26.4. The Mössbauer spectral data indicate the thermal hysteresis. However, the hysteresis width is somewhat different from the $T_{1/2\uparrow}$ and $T_{1/2\downarrow}$ values determined by the magnetic behavior, as shown in Figure 5. We can consider that the $T_{1/2\uparrow}$ and $T_{1/2\downarrow}$ in the Mössbauer results shifts to lower and higher temperatures, respectively, because the Mössbauer measurements require a longer time (a few days per measurement) than magnetic measurements (several dozen seconds per measurement). The behavior indicates a partial time-dependent relaxation from the metastable HS (LS) state to the LS (HS) ground one in the cooling (warming) process.

Concluding Remarks. The solvent-free Fe(III) complex $[Fe^{III}(Him)_2hapen]AsF_6$ was synthesized. One of the imidazole groups of $[Fe^{III}(Him)_2hapen]^+$ is hydrogen-bonded to a

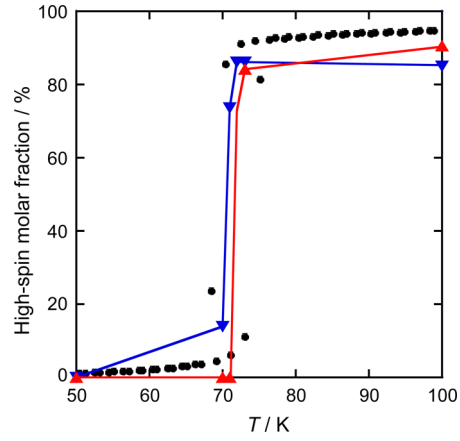

Figure 5. Molar fraction of HS vs total Fe^{III} in the cooling (blue ▼) and warming (red ▲) modes obtained by deconvolution analysis of the Mössbauer spectra, together with the molar fraction n_{HS} obtained from the magnetic susceptibility measurements (black ●). n_{HS} was calculated by using the equation $(\chi_M T)_{obs} = n_{HS}(\chi_M T)_{HS} + (1 - n_{HS})(\chi_M T)_{LS}$, with $(\chi_M T)_{HS}$ = 4.55 cm^3 K mol^{-1} and $(\chi_M T)_{LS}$ = 0.55 cm^3 K mol^{-1} as limiting values.

phenoxo oxygen atom of hapen of the adjacent unit to give a hydrogen-bonded 1D structure running along the *b*-axis. The temperature dependencies of the magnetic susceptibilities and Mössbauer spectra revealed an abrupt spin transition between the HS (S = 5/2) and LS (S = 1/2) states, with a small thermal hysteresis. The 1D chains exhibiting rod-like shape are stacked along the *b*-axis, and the anions occupy the space among the 1D chains. The anions are not hydrogen-bonded to the imidazole group of the 1D chain, suggesting that each 1D chain behaves as a spring and shrinks along the *b*-axis during the spin transition.[20] This work demonstrates that the SCO Fe^{III} complex can produce an abrupt spin transition and hysteresis when the hydrogen bonding is well-organized.

■ ASSOCIATED CONTENT

Ⓢ Supporting Information

Mössbauer spectra (Figure S1), Mössbauer data (Table S1), and crystallographic data in CIF format. This material is available free of charge via the Internet at http://pubs.acs.org. CCDC 926684 contains the supplementary crystallographic data for $[Fe^{III}(Him)_2(hapen)]AsF_6$. These data can be obtained free of charge from The Cambridge Crystallographic Data Centre via www.ccdc.cam.ac.uk/data_request/cif.

■ AUTHOR INFORMATION

Corresponding Author

*E-mail: naohide@aster.sci.kumamoto-u.ac.jp.

Notes

The authors declare no competing financial interest.

■ ACKNOWLEDGMENTS

T.F. was supported by the Research Fellowship for Young Scientists of the Japan Society for the Promotion of Science, KAKENHI 00248556.

■ REFERENCES

(1) (a) *Spin Crossover in Transition Metal Compounds I–III: Topics in Current Chemistry*; P. Gütlich, Goodwin, H. A., Eds.; Springer: New York, 2004. (b) Goodwin, H. A. *Coord. Chem. Rev.* **1976**, *18*, 293–325. (c) König, E. *Prog. Inorg. Chem.* **1987**, *35*, 527–623. (d) Gütlich, P.;

Hauser, A. *Coord. Chem. Rev.* **1990**, *97*, 1−22. (e) König, E. *Struct. Bonding (Berlin, Ger.)* **1991**, *76*, 51−152. (f) Gütlich, P.; Hauser, A.; Spiering, H. *Angew. Chem., Int. Ed. Engl.* **1994**, *33*, 2024−2054. (g) Real, J. A.; Gaspar, A. B.; Munoz, M. C. *Dalton Trans.* **2005**, 2062−2079. (h) Sato, O.; Tao, J.; Zhang, Y.-Z. *Angew. Chem., Int. Ed.* **2007**, *46*, 2152−2187. (i) Gütlich, P.; Gaspar, A. B.; Garcia, Y. *Beilstein J. Org. Chem.* **2013**, *9*, 342−391. (j) Linares, J.; Codjovi, E.; Garcia, Y. *Sensors* **2012**, *12*, 4479−4492.

(2) (a) Kröber, J.; Codjovi, E.; Kahn, O.; Grolière, F.; Jay, C. *J. Am. Chem. Soc.* **1993**, *115*, 9810. (b) Kahn, O.; Martinez, C. J. *Science* **1998**, *279*, 44−48. (c) Garcia, Y.; Kahn, O.; Rabardel, L.; Chansou, B.; Salmon, L.; Tuchaugues, J.-P. *Inorg. Chem.* **1999**, *38*, 4663−4670. (d) Galet, A.; Munoz, M. C.; Gaspar, A. B.; Real, J. A. *Inorg. Chem.* **2005**, *44*, 8749−8755. (e) Roubeau, O. *Chem.—Eur. J.* **2012**, *18*, 15230−15244. (f) Baldé, C.; Bauer, W.; Kaps, E.; Neville, S.; Desplanches, C.; Chastanet, G.; Weber, B.; Létard, J. F. *Eur. J. Inorg. Chem.* **2013**, 2744−2750. (g) Nowak, R.; Bauer, W.; Ossiander, T.; Weber, B. *Eur. J. Inorg. Chem.* **2013**, 975−983.

(3) (a) Létard, J.-F.; Guionneau, P.; Codjovi, E.; Lavastre, O.; Bravic, G.; Chasseau, D.; Kahn, O. *J. Am. Chem. Soc.* **1997**, *119*, 10861−10862. (b) Zhong, Z. J.; Tao, J.-Q.; Yu, Z.; Dun, C.-Y.; Lui, Y.-J.; You, X.-Z. *J. Chem. Soc., Dalton Trans.* **1998**, 327−328. (c) Hayami, S.; Gu, Z.-Z.; Yoshiki, H.; Fujishima, A.; Sato, O. *J. Am. Chem. Soc.* **2001**, *123*, 11644−11650. (d) Hagiwara, H.; Hashimoto, S.; Matsumoto, N.; Iijima, S. *Inorg. Chem.* **2007**, *46*, 3136−3143.

(4) (a) Boinnard, D.; Bousseksou, A.; Dworkin, A.; Savariault, J.-M.; Varret, F.; Tuchaugues, J.-P. *Inorg. Chem.* **1994**, *33*, 271−281. (b) Galet, A.; Gaspar, A. B.; Munoz, M. C.; Real, J. A. *Inorg. Chem.* **2006**, *45*, 4413−4422. (c) Neville, S. M.; Moubaraki, B.; Murray, K. S.; Kepert, C. J. *Angew. Chem.* **2007**, *119*, 2105−2108; *Angew. Chem., Int. Ed.* **2007**, *46*, 2059−2062. (d) Sato, T.; Nishi, K.; Iijima, S.; Kojima, M.; Matsumoto, N. *Inorg. Chem.* **2009**, *48*, 7211−7229. (e) Nishi, K.; Matsumoto, N.; Iijima, S.; Halcrow, M. A.; Sunatsuki, Y.; Kojima, M. *Inorg. Chem.* **2011**, *50*, 11303−11305. (f) Fujinami, T.; Nishi, K.; Matsumoto, N.; Iijima, S.; Halcrow, M. A.; Sunatsuki, Y.; Kojima, M. *Dalton Trans.* **2011**, *40*, 12301−12309. (g) Nishi, N.; Kondo, H.; Fujinami, T.; Matsumoto, N.; Iijima, S.; Halcrow, M. A.; Sunatsuki, Y.; Kojima, M. *Eur. J. Inorg. Chem.* **2013**, 927−933.

(5) Jäger, E.-G.; Hussler, E.; Rudolph, M.; Rost, M. *Z. Anorg. Allg. Chem.* **1985**, *525*, 67−85.

(6) Weber, B.; Bauer, W.; Obel, J. *Angew. Chem., Int. Ed.* **2008**, *47*, 10098−10101.

(7) (a) Fukukai, T.; Yabe, K.; Ogawa, Y.; Matsumoto, N.; Mrozinski, J. *Bull. Chem. Soc. Jpn.* **2005**, *78*, 1484−1486. (b) Tanimura, K.; Kitashima, R.; Brefuel, N.; Nakamura, M.; Matsumoto, N.; Shova, S.; Tuchagues, J. P. *Bull. Chem. Soc. Jpn.* **2005**, *78*, 1279−1282.

(8) (a) Nishida, Y.; Oshio, S.; Kida, S. *Chem. Lett.* **1975**, 79−80. (b) Nishida, Y.; Oshio, S.; Kida, S. *Bull. Chem. Soc. Jpn.* **1977**, *50*, 119−122. (c) Nishida, Y.; Kino, K.; Kida, S. *J. Chem. Soc., Dalton Trans.* **1987**, 1157−1161.

(9) (a) Ewald, A. H.; Martin, R. L.; Ross, I. G.; White, A. H. *Proc. R. Soc. London* **1984**, *A280*, 235−237. (b) Harris, G. *Theor. Chim. Acta* **1966**, *5*, 379−397. (c) Zerner, M.; Gouterman, M.; Kobayashi, H. *Theor. Chim. Acta* **1966**, *6*, 363−400.

(10) (a) Collman, J. P.; Sorrell, T. N.; Hodgson, K. O.; Kulshrestha, A. K.; Strouse, C. E. *J. Am. Chem. Soc.* **1977**, *99*, 5180−5181. (b) Collman, J. P.; Zhang, X.; Wong, K.; Brauman, J. I. *J. Am. Chem. Soc.* **1994**, *116*, 6245−6251. (c) Busch, D. H.; Alcock, N. W. *Chem. Rev.* **1994**, *94*, 585−623. (d) Scheidt, W. R.; Geiger, D. K.; Hayes, R. G.; Lang, G. *J. Am. Chem. Soc.* **1983**, *105*, 2625−2632. (e) Geiger, D.; Lee, Y. J.; Scheidt, W. R. *J. Am. Chem. Soc.* **1984**, *106*, 6339−6343.

(11) (a) Matsumoto, N.; Kimoto, K.; Nishida, K.; Ohyoshi, A.; Maeda, Y. *Chem. Lett.* **1984**, 479−480. (b) Matsumoto, N.; Kimoto, K.; Ohyoshi, A.; Maeda, Y. *Bull. Chem. Soc. Jpn.* **1984**, *57*, 3307−3311. (c) Matsumoto, N.; Ohta, S.; Yoshimura, C.; Kohata, S.; Okawa, H.; Maeda, Y.; Ohyoshi, A. *J. Chem. Soc., Dalton Trans.* **1984**, 2575−2584.

(12) Kennedy, B. J.; McGrath, A. C.; Murray, K. S.; Skelton, B. W.; White, A. H. *Inorg. Chem.* **1987**, *26*, 483−495.

(13) Hernandenz-Molia, R.; Mederis, A.; Dominguez, S.; Gili, P.; Ruiz-Perez, C.; Castineiras, A.; Solans, X.; Lloret, F.; Real, J. A. *Inorg. Chem.* **1998**, *37*, 5102−5108.

(14) Koike, M.; Murakami, K.; Fujinami, T.; Nishi, K.; Matsumoto, N.; Sunatsuki, Y. *Inorg. Chim. Acta* **2013**, *399*, 185−192.

(15) Nakao, N.; Nonagase, N.; Nakahara, A. *Bull. Chem. Soc. Jpn.* **1969**, *42*, 452−456.

(16) Kahn, O. *Molecular Magnetism;* VCH: Weinheim, Germany, 1993.

(17) MossWinn—Mössbauer spectrum analysis and database software. http://www.Mosswinn.com/. (Accessed Oct 10, 2013).

(18) (a) SIR92 Altomare, A.; Cascarano, G.; Giacovazzo, C.; Guagliardi, A.; Burla, M.; Polidori, G.; Camalli, M. *J. Appl. Crystallogr.* **1994**, *27*, 435. (b) Beurskens, P. T.; Admiraal, G.; Beurskens, G.; Bosman, W. P.; R. de Gelder, Israel, R.; Smits, J. M. M. *The DIRDIF-99 Program System;* Technical Report for the Crystallography Laboratory, University of Nijmegen: The Netherlands, 1999.

(19) *CrystalStructure 4.0: Crystal Structure Analysis Package;* Rigaku Corporation: Tokyo, Japan, 2010.

(20) Boukheddaden, K.; Miyashita, S.; Nishino, M. *Phys. Rev. B* **2007**, *75*, 094112.